Reexamination of string phase and shear thickening in simple fluids

Jerome Delhommelle,[1] J. Petravic,[2] and Denis J. Evans[2]
[1]*Equipe de Chimie et Biochimie Théoriques, UMR 7565, Université Henri Poincaré Nancy I, Boîte Postale 239, F-54506 Vandoeuvre-lès-Nancy, France*
[2]*Research School of Chemistry, The Australian National University, Canberra, ACT 0200, Australia*
(Received 18 March 2003; revised manuscript received 9 June 2003; published 3 September 2003)

In 1984, Erpenbeck observed a shear-induced alignment of particles into strings in nonequilibrium molecular dynamics simulations of hard spheres. Since then, it has remained unclear if this effect was genuine or if it arose from the use of a thermostat which assumed an incorrect form for the velocity profile. All studies performed up to now have focused on improving the accuracy with which the velocity profile is determined. We propose here a radically different approach: we apply a recently developed configurational expression for the temperature. This expression does not require any knowledge of the streaming velocity profile. Using a configurational thermostat, we show that the string phase is an artifact and we observe a shear-thickening regime, as seen in experiments on concentrated ''hard-sphere''-like colloidal dispersions.

DOI: 10.1103/PhysRevE.68.031201 PACS number(s): 66.20.+d, 02.70.Ns

I. INTRODUCTION

In 1984, Erpenbeck [1] observed an alignment of particles along the direction of the flow in nonequilibrium molecular dynamics (NEMD) simulations of planar Couette flow of a simple fluid. This new phase, known as ''string phase'' has drawn considerable interest and many NEMD studies have been carried out [2–14] since then. However, these studies have led to contradictory conclusions and it is still unclear whether the string phase is just a numerical artifact or whether it really exists.

A reason why this controversy is still not settled lies in the difficulty of making a connection between the NEMD results and experimental results. If the particles considered in NEMD simulations are meant to model argon atoms, the shear rates studied in those simulations are of the order of 10^{12} Hz, orders of magnitude beyond the shear rates accessible by experiments. A simple bulk liquid under increasing shear exhibits instabilities leading to turbulence in the linear response range of shear rates. The instability occurs at large Reynolds numbers, and in a system consisting of a large number of particles (of the order of the Avogadro number) this is attained for shear rates much lower than those within reach of computer simulations. Systems studied by simulation consist typically of several hundred particles in periodic boundary conditions. This imposes a lower limit on the wave vector describing collective motion and prevents large-scale instabilities. The Reynolds number is low even for extremely high shear rates, and one observes a non-Newtonian instead of turbulent behavior. NEMD results have therefore been often compared to experimental data obtained for colloidal dispersions, where the reduced shear rates used in simulations translate into the experimentally attainable values. Indeed, if the particles are meant to model a colloid such as poly (methyl methacrylate) (PMMA), the shear rates considered in NEMD are of the order of 10^2 Hz and thus of relevance for physical applications. At low (in the molecular dynamics sense) shear rates, all NEMD studies show some shear-induced ordering, associated with shear thinning (a decrease in apparent viscosity as the applied shear rate is increased) as experimentally observed in ''hard-sphere''-like colloidal suspensions [15]. At high shear rates, recent experiments [16] on such suspensions as well as Stokesian dynamics simulations [17] indicate an opposite behavior, i.e., shear thickening (a large increase in apparent viscosity when the applied shear rate is larger than a critical value). However, while these results are an indication of what may occur in a microscopic sample of a simple liquid, it is not possible to make a direct connection between the NEMD results and results for colloidal suspensions. Colloidal particles are suspended in a liquid, omitted in NEMD simulations, and the liquid-mediated hydrodynamic interactions affect the rheological behavior of the system. Nevertheless, there are enough similarities between NEMD for simple liquids and nonequilibrium Brownian dynamics (NEBD) simulations to indicate that some aspects of NEMD results are relevant for colloidal suspensions.

The NEMD method used in all the studies of simple liquids employs homogeneous shear fields [18] together with appropriate periodic boundary conditions [19]. This method correctly describes an isolated bulk system under arbitrarily strong shear [18]. However, adiabatic shearing causes a monotonic increase in internal energy. The system heats up and there is no well-defined final steady state from which transport coefficients can be calculated. In reality, viscous heat is dissipated to the environment through container walls. A realistic simulation of a bulk liquid system with macroscopic walls is beyond the reach of computer simulation. One can only simulate thin films of liquid between walls, where the confinement effects are still important. If the wall separation is sufficiently large, non-negligible temperature gradients would exist only close to the walls, and the temperature is approximately constant in the middle region. The purpose of the bulk NEMD simulations is to reproduce the behavior in this middle region between macroscopically separated walls, where temperature is approximately uniform and the system is sheared homogeneously. The same type of reasoning is used in all nonequilibrium simulations, including NEBD.

Constant temperature in NEMD simulations is achieved

by adding a ''thermostat term'' to the equations of motion, in order to account for the averaged effects of the natural heat dissipation processes in a homogeneous way. The results obtained by Liem *et al.* [20] showed the validity of this approach to model a fluid undergoing shear flow. They studied an atomic fluid sheared by two thermostatted walls and compared the results so obtained to those obtained using a thermostatted shear flow algorithm. They found that both methods generate indistinguishable results up to the maximum flow rates that are possible in a wall thermostatted system, and concluded that thermostatted NEMD was a satisfactory description of atomic fluids undergoing shear flow for low and moderate flow rates. In order to reproduce the desired temperature in Brownian dynamics of colloid dispersions, thermostat is replaced by drag and random forces, connected through the fluctuation-dissipation theorem. In this case, the heat transfer is assumed to be first between the solvent and the dispersed particles, and then implicitly through the container walls.

In all the previous NEMD studies mentioned above [2–14], as well as in NEBD simulations, the temperature T is evaluated according to

$$T=\frac{\left\langle \sum_{i=1}^{N} m[\mathbf{v_i}-\mathbf{u}(\mathbf{r_i},t)]^2 \right\rangle}{dNk_B}, \tag{1}$$

where N is the number of particles of the system, d is the number of Cartesian dimensions, k_B is the Boltzmann constant, m is the mass of a particle, $\mathbf{r_i}$ and $\mathbf{v_i}$ its position and velocity, and $\mathbf{u}(\mathbf{r},t)$ is the local flow or streaming velocity at position $\mathbf{r}$ at time t. At high Reynolds numbers, this streaming velocity is not generally known.

The random force in NEBD is only a zero mean random variable when the velocity of the Brownian particle is measured with respect to the local streaming velocity of the solvent,

$$m\frac{d[\mathbf{v_i}-\mathbf{u}(\mathbf{r_i},t)]}{dt}=-\zeta[\mathbf{v_i}-\mathbf{u}(\mathbf{r_i},t)]+\mathbf{F}_R, \tag{2}$$

where $\mathbf{F}_R$ is the random force, ζ is the friction coefficient, and $\mathbf{u}(\mathbf{r},t)$ is the local solvent velocity. At high flow rates Brownian dynamics (BD) offers no way to calculate the solvent flow velocity, because explicit reference to the solvent has been removed in order to efficiently calculate the motion of the Brownian particle.

Assumptions made concerning the form of the streaming velocity profile account for differences between all these previous studies. At low Reynolds number, the streaming velocity profile of planar Couette flow is linear. For sufficiently high Reynolds numbers, hydrodynamic stability theory applied to the momentum balance equation predicts that this profile will become unstable [21]. First, there will be a ''secondary'' profile superimposed on the initial linear profile, consisting of a mean part (of sinusoidal form in a NEMD simulation) and a fluctuating part. The secondary flow is present both in the flow direction and in the directions perpendicular to it. With further increase in the Reynolds number, the amplitude of the mean part would decrease and the amplitude of the fluctuating part would increase, leading to complete instability of the linear flow profile. With the appearance of the fluctuating secondary flow, the space and time dependences of streaming velocity are not known and therefore it needs to be calculated after each simulation step. In a simulation, there is no unique way to decide which part of particle velocity corresponds to local (in time and space) flow, and which to thermal motion. This again applies both to NEMD and NEBD simulations. The thermostatting mechanism (either the thermostat term or the combination of drag and random forces) will interpret any deviations from the assumed flow velocity profile as excess heat and remove it, thus constraining the flow velocity profile to the assumed form. Therefore, thermostatting the local kinetic temperature can lead to artificial flow profiles and hence to incorrect results.

An example of a huge qualitative thermostat-dependent difference in the behavior of a system under a strong perturbation is the emergence of a ''string phase'' in some simulations of strongly sheared simple liquids. Erpenbeck [1] assumed that even for high shear rates planar Couette flow characterized by a linear flow profile would be stable. However, at sufficiently high shear rates this assumption must break down. Evans and Morriss [4] showed that a thermostat relying on this assumption—a profile-biased thermostat (PBT)—led to the formation of string phase. They also showed that using a profile-unbiased thermostat (PUT), in which the streaming velocity is evaluated locally and at each time step, destroyed the string phase. On the other hand, as pointed out by Bagchi *et al.* [13], a PUT might also interpret the generation of heat as ''instantaneous'' secondary flows. Several mechanisms of PUT have been proposed over the past 15 years for atomic fluids and molecular fluids composed of short chains. Contradictory conclusions have been drawn: while some studies support the existence of a string phase [5,9,13], others show that using PUT destabilized the string phase [4,10,12]. Even more puzzling, Gray *et al.* [14] recently showed that constraining the velocity profile to a linear form was neither necessary nor sufficient for the string phase to occur: ''a necessary condition for positional ordering to occur is that the motion in the velocity gradient direction must be thermostatted.''

We reexamine this problem using a radically different approach. Instead of trying to devise a better PUT, we control the recently developed configurational expression for the temperature [22,23]. This expression allows the calculation of temperature solely from configurational quantities, such as first and second spatial derivatives of the interaction energy. No knowledge of streaming velocity profile is required, and therefore there is no need to distinguish between the streaming and thermal motion of particles. Temperature is evaluated according to

$$\frac{1}{k_BT}=\frac{\left\langle \sum_{i=1}^{N} \frac{\partial^2\Phi_0}{\partial \mathbf{r_i}^2} \right\rangle}{\left\langle \sum_{i=1}^{N} \left(\frac{\partial\Phi_0}{\partial \mathbf{r_i}} \right)^2 \right\rangle}, \tag{3}$$

where Φ_0 is the potential energy of the system. This expression can be used to devise a purely configurational thermostat for atomic or molecular fluids, possibly undergoing arbitrary flow [24,25].

In equilibrium, the kinetic and configurational expressions for the temperature are equivalent and can be derived from the thermodynamic temperature definition as the inverse rate of change of entropy with internal energy at constant volume, using Gibbs microscopic expression for entropy. Extending both kinetic and configurational definitions to systems out of equilibrium implies the approximation that the phase space probability distribution stays equal to the equilibrium probability distribution in a reference frame comoving with the flow, i.e., the assumption of local equilibrium is valid. This is assumed in both types of temperature definitions when used out of equilibrium, otherwise temperature would not be a well-defined quantity. However, the configurational expression is free from errors associated with an incorrect estimate of flow velocity, and therefore can be considered as ''more correct.''

II. SIMULATION METHOD

We studied three different systems, referred to as *A*, *B*, and *C* in the text. In all simulations, we used a reduced system of units, where the unit of mass is the mass of the particle *m*, unit of energy is the characteristic energy ε of the pair potential, and the unit of length is the particle exclusion diameter σ. System *A* is a two-dimensional (2D) system of 896 soft disks as in Ref. [4] with the pair interaction potential $\phi(r)=4\varepsilon(\sigma/r)^{12}$, at the reduced temperature $T^*=k_BT/\varepsilon=1$ and at the reduced number density $\rho^*=\rho\sigma^3=0.9238$. System *B* is a three-dimensional system of 1000 Lennard-Jones particles; interaction potential $\phi(r)=4\varepsilon[(\sigma/r)^{12}-(\sigma/r)^6]$ near the triple point, $T^*=0.722$ and $\rho^*=0.844$. The particles of system *C* interact through the combination of soft sphere and screened Coulomb interaction of Ref. [5], $\phi(r)=\varepsilon(\sigma/r)^{12}+\{[1-(r/r_{cut})]^2/r\}$ at $T^*=0.25$ and $\rho^*=0.84$ ($r_{cut}=2.5\sigma$ is the cutoff radius). We studied two system sizes. In the system $C1$ the number of particles was 512, and in system $C2$ there were 4096 particles.

The NEMD method used in this work is the homogeneous Sllod algorithm (so named because of its close relationship to the Dolls tensor algorithm) [18], in which the shear rate is introduced in the equations of motion as a mechanical perturbation. For adiabatic Couette flows, the Sllod equations are exact regardless of Reynolds number. This is because adiabatic Sllod is equivalent to Newton's equations for $t>0$ applied to an initial distribution of states which is in local thermodynamic equilibrium for planar Couette flow, regardless of any instabilities in the linear velocity profile. NEMD simulations were run with two types of thermostats: (1) a PBT thermostat based on the expression given by Eq. (1) for the temperature and (2) a configurational thermostat based on the expression given by Eq. (2). When the imposed streaming velocity is parallel to the *x* axis, with the imposed velocity gradient along the *y* axis, the PBT thermostatted equations of motions reduce to [18]

$$\dot{\mathbf{r}}_i=\frac{\mathbf{p}_i}{m}+\gamma y_i\mathbf{e}_x,$$

$$\dot{\mathbf{p}}_i=\mathbf{F}_i-\gamma p_{y_i}\mathbf{e}_x-\xi\mathbf{p}_i, \tag{4}$$

where ξ is the thermostatting multiplier given by Gauss' principle of least constraint,

$$\xi=\frac{\sum_i(\mathbf{F}_i\cdot\mathbf{p}_i-\gamma p_{x_i}p_{y_i})}{\sum_i\mathbf{p}_i\cdot\mathbf{p}_i}. \tag{5}$$

The configurationally thermostatted equations of motions are [24,25]

$$\dot{\mathbf{r}}_i=\frac{\mathbf{p}_i}{m}+\gamma y_i\mathbf{e}_x+\frac{s}{T}\frac{\partial T_{conf}}{\partial\mathbf{r}_i},$$

$$\dot{\mathbf{p}}_i=\mathbf{F}_i-\gamma p_{y_i}\mathbf{e}_x, \tag{6}$$

$$\dot{s}=-Q\frac{(T_{conf}-T)}{T}.$$

In these equations, $\mathbf{r}_i$ and $\mathbf{p}_i$ are the position and ''peculiar'' momentum (i.e., with respect to linear streaming velocity profile $\gamma y_i\mathbf{e}_x$) of particle *i*, $\mathbf{F}_i$ is the Newtonian force exerted on *i*, and *m* its mass. *T* is the imposed temperature while T_{conf} is the value given by Eq. (2) [*Q* is a damping constant set to $10(m\sigma^4/\varepsilon)$]. $\gamma=[du_x(y)/dy]$ is the imposed shear rate and $\mathbf{e}_x$ is an unit vector along the *x* axis. For thermostatted flows, the momenta $\mathbf{p}_i$ are peculiar with respect to the actual velocity profile only for low Reynolds number flows where the streaming velocity is $\gamma y_i\mathbf{e}_x$ [see Eqs. (4) and (6)]. Thus Eq. (4) is only correct for sufficiently small Reynolds numbers. Equation (6), on the other hand, makes no assumption about the streaming velocity profile. The equations of motion were integrated using a fourth-order Gear predictor-corrector algorithm with a time step $\tau^*=\tau(1/\sigma)\sqrt{\varepsilon/m}=0.001$, except for the highest shear rates where a smaller time step had to be used. The shear viscosity is evaluated as the ratio $-P^*_{xy}/\gamma^*$, where $P^*_{xy}=P_{xy}\sigma^2/\varepsilon$ for the 2D system and $P^*_{xy}=P_{xy}\sigma^3/\varepsilon$ for the 3D systems, which denotes the corresponding element of the pressure tensor and $\gamma^*=\gamma\sigma\sqrt{m/\varepsilon}$ is the reduced shear rate. The kinetic part of P^*_{xy} is evaluated by subtracting the linear streaming velocity profile for a planar Couette flow. When the actual profile was found to differ from the linear form, we found that subtracting the assumed linear profile or the actual profile yielded the same numerical value for the shear viscosity. The reason for this is that the kinetic part of all the elements of the pressure tensor is much smaller than the potential part at the densities investigated in this work.

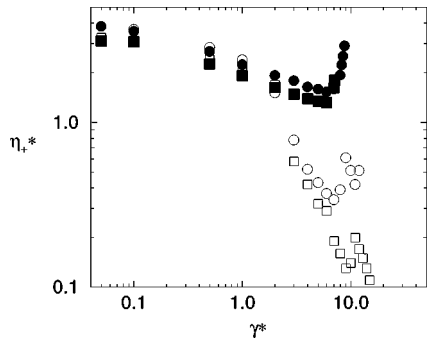

FIG. 1. Shear viscosity as a function of shear rate for the 2D soft disks system (circles) and the 3D Lennard Jones system (squares). Results obtained using a PBT thermostat are plotted as open symbols while results obtained with a configurational thermostat are plotted as filled symbols.

III. RESULTS AND DISCUSSION

Shear viscosity is plotted against shear rate for systems *A* and *B* in Fig. 1. Both thermostats result in similar shear viscosities under low to moderate shear for both fluids: we observe a decrease in shear viscosity, i.e., shear thinning associated with shear-induced ordering in the fluid. This effect is observed in all simulations and with all types of thermostats, profile biased or not. Shear thinning is an effect experimentally observed in many more complex systems (e.g., colloidal suspensions), where particles are of larger size and Reynolds number is low even for high shear rates. Despite the difference between the interactions in these systems and simple liquids, it is accepted that simple liquids would indeed be shear thinning if it were possible to perform experiments on sufficiently small-sized samples and at sufficiently high shear rates.

Dramatic differences appear at high shear rates for the two systems. When a PBT is used, shear viscosity exhibits a sharp drop associated with the onset (at approximately $\gamma^* = 2.5$) of positional ordering within the fluid (the "string phase") as plotted in Fig. 2(a). We point out that thermodynamic quantities such as pressure and energy also exhibit a sharp drop at this value of the shear rate. For higher shear rates, shear viscosity remains very low, even for very high shear rates $\gamma^* > 10$. Note that shear viscosity is not a monotonic function of shear rate after the drop: an inspection of the configurations obtained for those shear rates indicates coexisting liquid and string phases [6]. In all cases where the simulations show the development of a string phase, they were done with a thermostat that is in some way profile biased, i.e., constrains at least some components of streaming velocity to an assumed linear form. This is true both for NEMD [5,9,13] and NEBD results [7].

Results obtained using a configurational thermostat are very different. Shear viscosity decreases steadily until a given shear rate (approximately $\gamma^* = 6$ for system *A* and $\gamma^* = 7$ for system *B*) and then increases dramatically for very high shear rates, as both fluids exhibit shear thickening, similarly to what was experimetally observed for concentrated hard-sphere-like colloidal suspensions [16]. No drop in any thermodynamic quantity is observed when a configurational thermostat is used: pressure and internal energy steadily increase with shear rate. In the shear-thickening regime [Fig. 2(b)], the fluid has the same disordered appearance as in the shear-thinning regime.

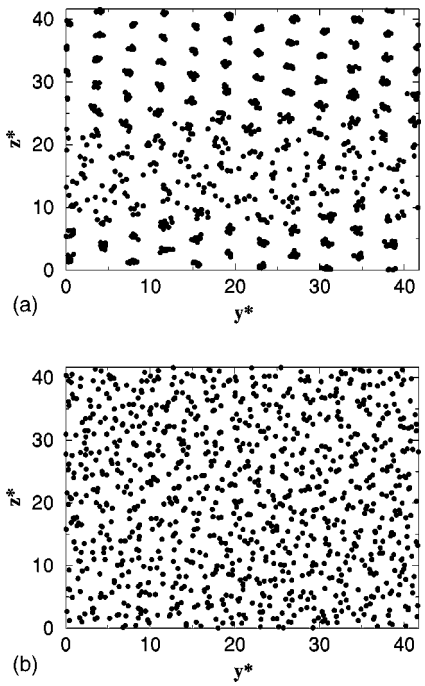

FIG. 2. Snapshots for the 3D Lennard Jones fluid with (a) a PBT thermostat $\gamma^* = 4$ and (b) a configurational thermostat at $\gamma^* = 7$. These figures show the view from the flow direction.

The PBT used in this work is biased in two ways. It not only imposes a linear-velocity profile in the direction of the flow, but it also prevents any deviation from a zero-velocity profile to appear in directions perpendicular to the flow direction. Unlike this PBT, the configurational thermostat does not interpret deviations from laminar flow as heat and thus does not suppress the development of secondary flows. We plot in Fig. 3 the deviations from the linear flow profile in the flow direction when a configurational thermostat is used for system *B* (note that with a PBT we observe that the strings are moving at the velocity of the imposed profile). Figure 3

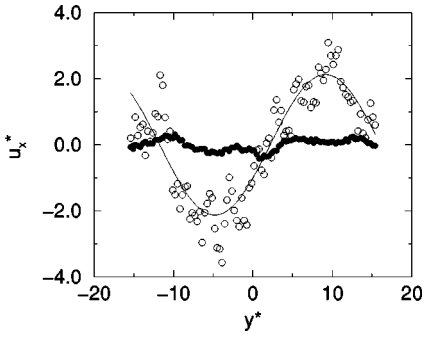

FIG. 3. Deviation of the velocity profile for the *x*-component (x being the direction of the flow) system along the velocity gradient direction from the linear form when using a configurational thermostat for a 3D Lennard-Jones fluid at $\gamma^* = 3$ (filled circles) and $\gamma^* = 5$ (open circles). Lines are sinusoidal fits.

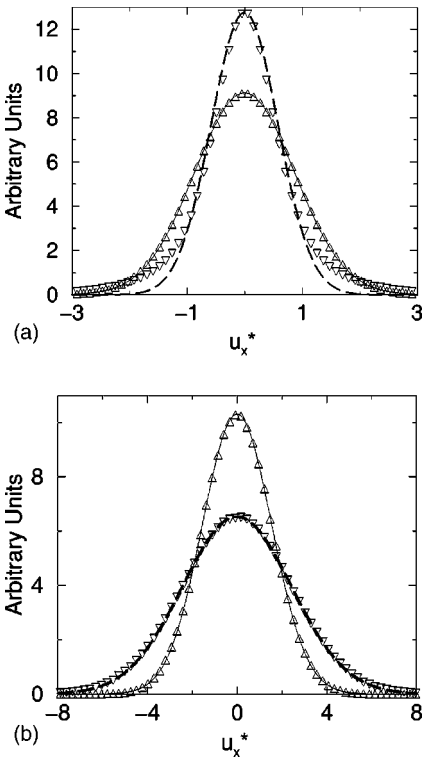

FIG. 4. Distribution function for the *x* component of the peculiar velocity profile for the 3D Lennard-Jones fluid (a) when using a PBT at $\gamma^*=2$ (triangles up) and $\gamma^*=5$ (triangles down) and (b) when using a configurational thermostat at $\gamma^*=3$ (triangles up) and $\gamma^*=5$ (triangles down). Fits to a Gaussian form are plotted as solid lines and dashed lines.

clearly shows that at high shear rates, a sinusoidal-like secondary flow profile is superimposed upon the linear flow profile as observed in laboratory experiments and predicted by hydrodynamics stability theory. (Note that the Lees-Edwards periodic boundary conditions ensure that the phase of this sinusoid is completely arbitrary.) In directions perpendicular to the flow direction, a PBT prevents any significant fluctuations from a flat profile from appearing. On the other hand, profiles obtained with a configurational thermostat exhibit strong fluctuations in those directions at high shear rates. This explains why no string phase appears with a configurational thermostat.

We have collected histograms of peculiar velocities for fluids undergoing shear flow using a PBT [Fig. 4(a)] or a configurational thermostat [Fig. 4(b)]. Fits to a Gaussian form are also plotted. The *x* components of peculiar velocities were calculated by subtracting the linear streaming velocity profile (for $\gamma^*=5$) with a configurational thermostat, subtraction of the linear profile yielded the same result as the subtraction of the linear profile and the sinusoidal fit shown in Fig. 4(b), because the amplitude of the sinusoidal part of the secondary flow is small compared to the amplitude of the fluctuating part and thermal motion. The distribution function obtained for the components of the peculiar velocities using a PBT follows the Maxwell law until the onset of the string phase and then deviates from the Gaussian shape. In contradistinction, when a configurational thermostat is used,

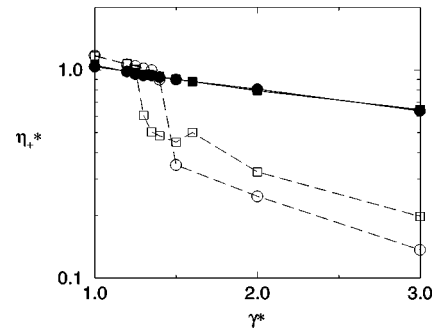

FIG. 5. Shear viscosity as a function of shear rate for the 3D colloidal system: 512 particles (circles) and 4096 particles (squares). Results obtained using a PBT are plotted as open symbols, while results obtained with a configurational thermostat are plotted as filled symbols.

these distribution functions remain Gaussian even at high shear rates as shown in Fig. 4(b). They are also broader as a result of the large velocity fluctuations—allowed by the use of a configurational thermostat–observed in the velocity profile in Fig. 3. The same conclusions hold for the *y* and *z* directions.

Finally, we present results obtained for a potential model used for colloidal suspensions [5]. The results obtained using the two types of thermostats are plotted for the two system sizes $C1$ (512 particles as in Ref. [6]) and $C2$ (4096 particles) in Fig. 5. Results obtained using a PBT exhibit system size dependence. We observe the onset of a string phase at a shear rate of 1.4 for system $C1$—in good agreement with the results of Ref. [6]—and at a shear rate of 1.3 for system $C2$. On the contrary, no such dependence on the system size is observed when a configurational thermostat is used. Once again, we do not observe any string phase but shear thickening for shear rates higher than 7.2 (not shown).

An intuitively acceptable explanation of the sudden qualitative change of behavior of the system at some critical shear rate in terms of heat transfer is that such a change, be it to a string phase or to a shear-thickening regime, occurs when the typical change in streaming velocity between nearest neighbors, $\langle|\Delta u_x|\rangle$, becomes comparable to the mean thermal velocity. Mean thermal velocities are equal to $\sqrt{k_B T_{kin}/m}$, where T_{kin} is evaluated according to Eq. (1). Since velocity fluctuations are limited with PBT, this means that shear thickening with configurational thermostat will occur at higher shear rates than string phase with PBT. This is the case in all investigated systems.

Let us first look at the PBT results and the ''string transition'' in more detail. In system *A* the nearest neighbor distance is $d_s^*=1.04$ and the mean velocity fluctuations are $\sqrt{k_B T_{kin}/m}\simeq 1.0$ in reduced units. The critical shear rate at which string phase appears is $\gamma_c^*=2.5$, and the mean change of streaming velocity between nearest neighbor layers is $\langle|\Delta u_x|\rangle = d_s^* \gamma_c^* \simeq 2.6$. In system *B*, the average nearest neighbor separation is 1.06, and velocity fluctuations are $\sqrt{k_B T_{kin}/m}=0.85$. String phase develops at the reduced shear rate of about 2.5, where the change of streaming velocity between nearest neighbor layers is $\langle|\Delta u_x|\rangle\simeq 2.7$

$\simeq 3\sqrt{k_B T_{kin}/m}$. In system *C*, the average nearest neighbor separation is 1.687, and velocity fluctuations are $\sqrt{k_B T_{kin}/m} = 0.5$. String phase develops at the reduced shear rate of about 1.5, where the change of streaming velocity between nearest neighbor layers is $\langle|\Delta u_x|\rangle \simeq 2.53 \simeq 5\sqrt{k_B T_{kin}/m}$

Shear-thickening results with configurational thermostat are also consistent with this explanation. The transition to the thickening regime in system *A* takes place at the shear rate of 6, where the kinetic temperature, given by Eq. (1), is equal to 8.91 and the average change of streaming velocity is $\langle|\Delta u_x|\rangle \simeq 6.24 \simeq 2\sqrt{k_B T_{kin}/m}$. In system *B*, the critical shear rate is around 7, and the corresponding kinetic temperature is 14.35. The difference in streaming velocities of the nearest neighbor layers is $\langle|\Delta u_x|\rangle \simeq 7.5 \simeq 2\sqrt{k_B T_{kin}/m}$. In system *C*, the critical shear rate is around 7.2 and the corresponding kinetic temperature is 5.98. The difference in streaming velocities of the nearest neighbor layers is $\langle|\Delta u_x|\rangle \simeq 12.15 \simeq 5\sqrt{k_B T_{kin}/m}$.

Shear thickening is observed in colloids at high shear rates [16]. In simulations, it is found even in the constrained linear profile laminar flow regime if hydrodynamic effects of solvent are taken into account [17]. It can be argued that if it were possible to include the deviations from the linear flow velocity profile in this simulation, it would further enhance shear thickening at very high shear rates. The actual experimentally observed result [16] is probably a consequence of a combination of both effects.

IV. CONCLUSION

We have applied a configurational thermostat to a simple fluid undergoing shear flow for very high shear rates. This method avoids making incorrect assumptions on the velocity profile under strong shear which lead to the onset of an artifact, the so-called string phase. Our approach successfully accounts for key features observed experimentally for high values of Reynolds number. In simulations of simple liquids with configurational (i.e., profile unbiased) thermostat, there is neither a sharp drop of viscosity nor any shear-induced order. The sinusoidal kink in all components of streaming velocity profile consistent with the stability arguments in Refs. [5] and [21] is observed, but at higher shear rates after shear thinning, because of small system size. After some critical shear rate the system shear thickens. We propose that a condition for a qualitative change of behavior with the increase of shear rate is that the typical differences in streaming velocity between nearest neighbors become larger than the mean thermal velocity of the particles, and the flow therefore becomes athermal. This conjecture is in good agreement for both the string phase and shear-thickening transitions. One system where it is always satisfied is, e.g., sheared sand, where thermal motion is negligible compared to flow motion because of the large mass and size of particles. This system is well known to be shear thickening for all values of shear rate. This can be regarded as an argument supporting a hypothesis that all systems would be shear thickening when our condition is satisfied, if the Reynolds number is sufficiently low for sufficiently high shear rates. In particular, simple liquids would shear thicken under strong shear in a viscometer of microscopic size. As shown in previous work [24,25], the configurational thermostat can be readily used to deal with any type of fluid (e.g., with either rigid or nonrigid internal degrees of freedom) undergoing any type of flow.

ACKNOWLEDGMENTS

The authors wish to thank the National Facility of Australian Partnership for Advanced Computing for a substantial allocation of computer time.

[1] J.J. Erpenbeck, Phys. Rev. Lett. **52**, 1333 (1984).
[2] L.V. Woodcock, Phys. Rev. Lett. **54**, 1513 (1985).
[3] D.M. Heyes, J. Chem. Soc., Faraday Trans. 2 **82**, 1365 (1986).
[4] D.J. Evans and G.P. Morriss, Phys. Rev. Lett. **56**, 2172 (1986).
[5] W. Loose and S. Hess, Rheol. Acta **28**, 91 (1989).
[6] T. Yamada and S. Nosé, Phys. Rev. A **42**, 6282 (1990).
[7] W. Xue and G.S. Grest, Phys. Rev. Lett. **64**, 419 (1990).
[8] M.J. Stevens, M.O. Robbins, and J.F. Belak, Phys. Rev. Lett. **66**, 3004 (1991).
[9] W. Loose and G. Ciccotti, Phys. Rev. A **45**, 3859 (1992).
[10] P. Padilla and S. Toxvaerd, J. Chem. Phys. **103**, 716 (1995).
[11] I. Borzsak and A. Baranyai, Phys. Rev. E **52**, 3997 (1995).
[12] K.P. Travis, P.J. Daivis, and D.J. Evans, J. Chem. Phys. **105**, 3893 (1996).
[13] K. Bagchi, S. Balasubramian, C.J. Mundy, and M.L. Klein, J. Chem. Phys. **105**, 11183 (1996).
[14] R.A. Gray, S. Chynoweth, Y. Michopoulos, and G.S. Pawley, Europhys. Lett. **43**, 491 (1998).
[15] B.J. Ackerson and P.N. Pusey, Phys. Rev. Lett. **61**, 1033 (1988).
[16] P. D'Haene, J. Mewis, and G.G. Fuller, J. Colloid Interface Sci. **156**, 350 (1993).
[17] J.R. Melrose, Faraday Discuss. **123**, 355 (2003).
[18] D. J. Evans and G. P. Morriss, *Statistical Mechanics of Nonequilibrium Liquids* (Academic Press, London, 1990).
[19] A.W. Lees and S.F. Edwards, J. Phys. C **5**, 1921 (1972).
[20] S.Y. Liem, D. Brown, and J.H.R. Clarke, Phys. Rev. A **45**, 3706 (1992).
[21] J.L. McWhirter, J. Chem. Phys. **118**, 2824 (2003).
[22] H.H. Rugh, Phys. Rev. Lett. **78**, 772 (1997).
[23] O.G. Jepps, G. Ayton, and D.J. Evans, Phys. Rev. E **62**, 4757 (2000).
[24] J. Delhommelle and D.J. Evans, J. Chem. Phys. **115**, 43 (2001).
[25] L. Lue, O.G. Jepps, J. Delhommelle, and D.J. Evans, Mol. Phys. **100**, 2387 (2002).